JOURNAL OF MATERIALS SCIENCE 21 (1986) 3884–3888

Stable crack growth in a surface compression-strengthened hollow cylinder

H. F. NIED
General Electric Company, Corporate Research and Development Center, Schenectady, New York 12301, USA

In this paper the static fatigue problem for a circumferentially cracked hollow cylinder is examined. For this particular configuration, stable crack growth, in the absense of any external forces, is determined for cylinders with axial components of residual stress which are compressive on the inner and outer radial surfaces and tensile in the cylinder wall. An initial surface crack which is deep enough to penetrate the compression strengthened surface region and enters the tensile zone may propagate in a stable manner until either sudden spontaneous failure occurs or the crack arrests. Since a portion of the crack near the cylinder surface will be closed because of the compressive residual stress field, an additional unknown in the problem is the extent of the crack surface contact. This crack surface contact length is determined by iteration on the integral equation which arises in the mathematical derivation for an embedded circumferential crack in a hollow cylinder. As an illustration of stable crack growth for this geometry with a realistic residual stress distribution, numerical results are presented for a hollow, soda-lime glass cylinder, based on crack growth rates in soda-lime glass exposed to water at 25° C. Using the fracture toughness and slow crack growth characteristics for soda-lime glass, the conditions for no crack propagation, crack propagation leading to crack arrest, and catastrophic failure are established.

1. Introduction

It is quite well-known that the impact and fatigue resistance of most brittle structures can be significantly improved by introducing residual stresses which are compressive at the material surface. For example, in glasses these residual stresses can be created by thermal tempering or ion exchange techniques. However, brittle materials strengthened in this fashion appear to be especially susceptible to spontaneous fracture even in the absence of any applied loads. Such failures can be explained by the stable crack growth behaviour of deep surface cracks which have penetrated the compression strengthened surface of the material and entered into the tensile stress region which exists for structures in a state of self-equilibrium. Surface cracks with depths sufficient to exhibit stable propagation in surface compression strengthened structures, usually have been introduced by foreign object impact or severe scratching of the surface.

The static fatigue behaviour of ceramics and glasses in corrosive environments [1–3] and in vacuum [4] have been extensively investigated. In these investigations careful experimental measurements were made to determine the crack velocity during subcritical crack growth under a variety of environmental and thermal conditions. This experimental information has in turn been utilized [5–7] in fracture analysis calculations which take into account extensive subcritical crack growth prior to catastrophic failure for externally loaded and thermally stressed structures. For situations concerned with static fatigue in the absence of any external loads, similar failure calculations can be performed as long as the interaction between the crack and the internal residual stress field is properly taken into account. In [8] such an analysis is performed for a surface compression strengthened glass plate.

In this paper an analysis similar to that given in [8] will be performed for a hollow circumferentially cracked cylinder (Fig. 1). The crack is axisymmetric and lies in a plane perpendicular to the cylinder axis. The crack may be either located on the inner radius or the outer radius of the cylinder. It is assumed that a parabolic residual stress distribution acting in the z-direction (Fig. 1) exists through the cylinder wall in the uncracked cylinder. This residual stress distribution realistically represents the type of stress field usually associated with thermal tempering. The magnitude of the residual stress on the inner and outer cylinder surfaces is given by σ_s. If a circumferential surface crack is introduced into this residual stress field, the crack will remain closed along its entire length as long as it is located entirely within the compressive region near the cylinder surface. However, if the crack tip enters the tensile region in the central portion of the cylinder wall, the crack will be cusp-shaped (Fig. 1) with a portion of the crack open (near the crack tip) and a portion of the crack closed.

2. Formulation of the crack problem

Solution of the problem depicted by Fig. 1 involves the general solution for an embedded axisymmetric circumferential crack in an infinitely long hollow

0022–2461/86 $03.00 + .12 © *1986 Chapman and Hall Ltd.*

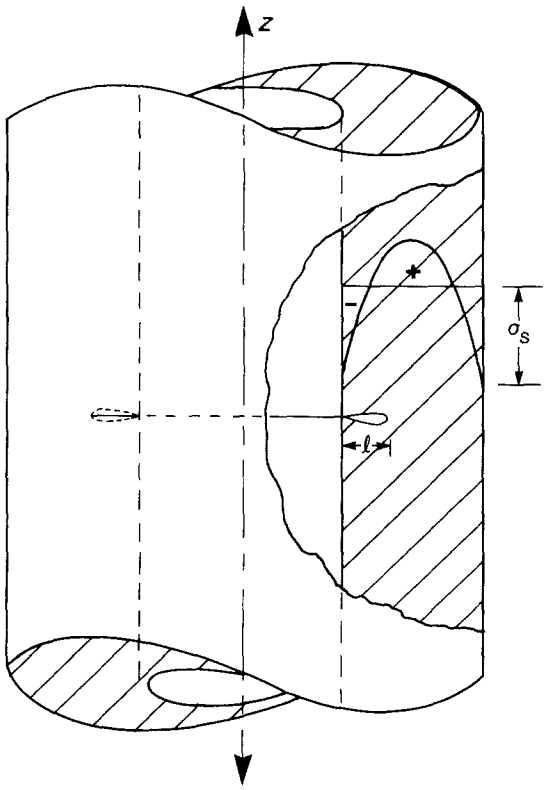

Figure 1 Hollow cylinder with an axisymmetric circumferential crack of length l. Parabolic residual stress distribution with surface magnitude σ_s.

cylinder (Fig. 2). The inner and outer radii of the cylinder are given by a and b, respectively, with the inner crack radius given by c and outer crack radius given by d. This problem has been solved for both symmetrical [9] and nonsymmetrical [10] axial stress distribution σ_z. For the axisymmetrical stress distribution, the mixed boundary value problem depicted by Fig. 2 results in an integral equation of the form

$$\int_c^d \left[\frac{1}{t-r} + k(r, t)\right] g(t)\mathrm{d}t = -\frac{1-\nu}{\mu}\pi\sigma_z(r) \quad (c < r < d) \tag{1}$$

where the unknown $g(r)$, is the derivative of the crack surface displacement in the axial z-direction given by

$$g(r) = \frac{\partial}{\partial r} u_z(r, 0^+) \quad (c < r < d) \tag{2}$$

In Equation 1, the Fredholm kernel $k(r, t)$ is a lengthy

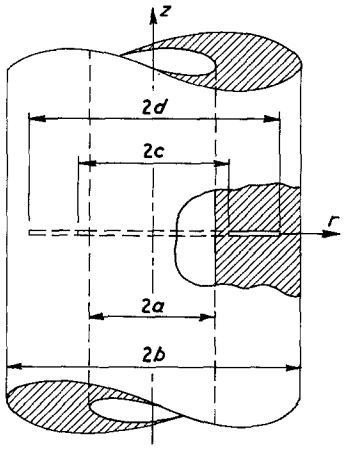

Figure 2 Geometry for a hollow cylinder with an embedded axisymmetric crack.

expression which is given in [9], ν is Poisson's ratio and μ is the elastic shear modulus. In the following analysis the stress σ_z will be the residual stress distribution denoted by σ_R which satisfies the equilibrium condition

$$\int_a^b \sigma_R(r) r\, \mathrm{d}r = 0 \tag{3}$$

If we assume a parabolic residual stress distribution through the cylinder wall, then the residual stress is given by

$$\sigma_z(r) = \sigma_R(r) = \sigma_s\left[\frac{6(r-a)(b-r)}{(b-a)^2} - 1\right] \tag{4}$$

where σ_s is the magnitude of the compressive stress on the surfaces of the cylinder (see Fig. 1). In addition to Equation 1, an auxiliary equation of the form

$$\int_c^d g(t)\, \mathrm{d}t = 0 \tag{5}$$

is necessary to assure single-valuedness of the solution for the embedded crack problem. The details concerning the reduction of Equations 1 and 5 to a system of algebraic equations and their subsequent numerical solution is given in [9] and will not be elaborated further here. It is sufficient to state that the stress intensity factors at both crack tips can be calculated very efficiently using these numerical methods.

The crack contact length in the compressive zone will be specified as ε and is an additional unknown. The physical condition which accounts for this unknown is the smooth closure condition of the crack surfaces at $r = a + \varepsilon$ or $r = b - \varepsilon$. Thus, the problem may be treated as an embedded crack problem with smooth closure assured by the condition

$$K(a + \varepsilon) = 0, \text{ or } K(b - \varepsilon) = 0 \tag{6}$$

where K is the usual stress intensity factor. In practice this condition is satisfied (for an internal edge crack) by fixing the location of the crack tip at $r = d$ (Fig. 2) and then determining the radial position r of the crack tip at c by iteration such that $K(c) = 0$. The solution for an external edge crack can be obtained in a similar manner, but in this case the position of the crack tip at $r = d$ is varied until $K(d) = 0$. In this manner the stress intensity factors for edge cracks of various depths are obtained from the solution of the embedded crack problem as well as the length of the crack contact zone ε.

Fig. 3 is a plot of the stress intensity factor solutions for internal and external circumferential edge cracks as a function of crack tip position r_0 normalized with respect of the cylinder wall thickness h ($h = b - a$). The crack length l is either given by $l = d - a$ or $l = b - c$, depending on whether the crack originates from the cylinder inner radius or outer radius. The residual stress field used to generate these solutions is the one given by Equation 4. In Fig. 3 the results are presented for two different $a:b$ ratios, $a:b = 0.9$ and $a:b = 0.7$. It can be seen that there is little difference between the magnitude of the stress intensity factors at $a:b = 0.9$ or $a:b = 0.7$. The main difference is seen in $a:b = 0.7$, where the maximum stress intensity factor for an external edge crack in this residual stress

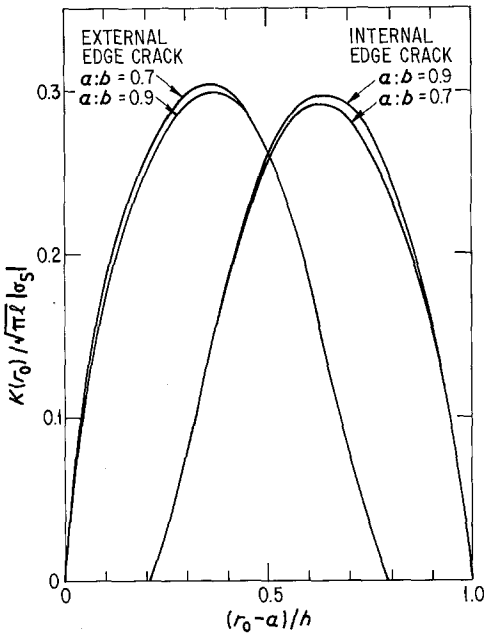

Figure 3 Stress intensity factors for internal and external edge cracks in a hollow cylinder subjected to parabolic residual stresses.

field is noticeably greater than it is for an internal edge crack. With decreasing $a:b$, as the wall thickness increases, this effect becomes even more evident. The stress intensity factor for the edge crack is zero while the crack is totally encompassed by the compressive region. However, once the crack tip has entered the tensile zone, the stress intensity factor increases rapidly, reaches a maximum and then decreases to zero as the crack reaches the other side of the cylinder.

Fig. 4 plots the value of the crack contact length ε corresponding to the stress intensity factor solutions given in Fig. 3 for circumferential cracks in a cylinder with an $a:b$ ratio of 0.9. The dashed line represents the crack length for cracks completely contained within the surface compression zone and simply increases linearly with increasing crack length. Once the crack tip completely penetrates this compressive region the contact length decreases with increasing crack length.

3. The static fatigue problem

With the stress intensity factors now known as a function of crack length l, it is possible to integrate empirical crack growth velocity expressions of the form

$$\frac{dl}{dt} = F(K) \tag{7}$$

to obtain the time to failure, provided that for the residual stress field of interest the value of the stress intensity factor K exceeds some minimum value K_T. The K_T (K threshold) values are known for many brittle materials and represent a K value below which no measurable crack growth can be detected. Thus, for a given internal residual stress state and an initial crack length l_i, $K(l_i) > K_T$ for any crack growth to take place. From the solution for K as a function of the crack length (Fig. 3), it is also possible to determine the minimum crack length necessary for any stable crack growth. This minimum crack length denoted by l_1 is determined from the condition

$$K(l_1) = K_T,\ K'(l_1) > 0 \tag{8}$$

After stable crack growth has been initiated, the crack will grow until either the critical stress intensity factor K_{IC} is reached and the cylinder fails in a catastrophic manner, or the stress intensity factor decreases as the crack approaches the opposite cylinder wall and the crack arrests. Denoting the crack lengths at which catastrophic failure or arrest occurs as l_2 and l_a, respectively, these two alternative conditions are determined from

$$K(l_2) = K_{IC} \tag{9}$$

$$K(l_a) = K_T,\ K'(l_a) < 0 \tag{10}$$

By utilizing conditions (Equations 8 to 10) it is possible to integrate Equation 7 to obtain the time for crack arrest

$$T_a = \int_{l_i}^{l_a} \frac{dl}{F(K)} \tag{11}$$

or catastrophic failure

$$T_f = \int_{l_i}^{l_2} \frac{dl}{F(K)} \tag{12}$$

Even though Equation 11 may be useful for estimating whether crack arrest will occur, in practice crack arrest will also depend on the maximum velocity the crack attains during the stable crack growth. That is, if the crack velocity becomes too great, the running crack may pass completely through the "back-side" compressive zone, even though the K value may dip below K_T. Since dynamic effects are neglected in this analysis, Equation 11 can be expected to hold only for those situations where the maximum K value does not come too close to K_{IC} (relatively low crack velocities). In these situations it is expected that dynamic effects will be negligible.

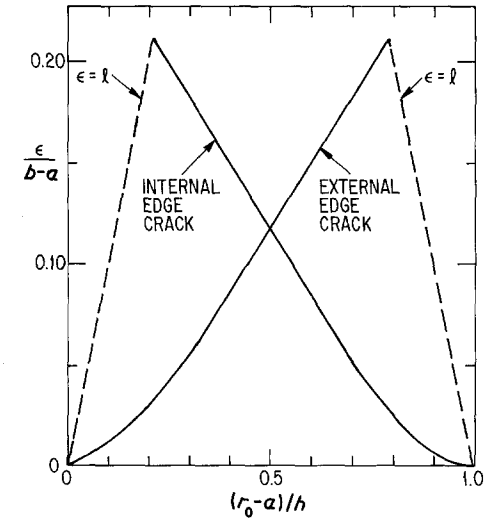

Figure 4 Crack contact length ε for a hollow cylinder with parabolic residual stresses. $a:b = 0.9$, $h = b - a$.

4. Numerical results

As a numerical example of stable crack growth for a circumferentially cracked hollow cylinder with a residual stress given by Equation 4, the static fatigue behaviour of soda-lime glass exposed to water at 25° C

will be used. In the following calculations the cylinder wall will be taken to have a thickness of 2 mm with an outer diameter of 4 cm. In addition it will be assumed that the circumferential crack originates on the inner radius of the hollow cylinder.

Experimental measurements of the slow crack growth velocities in soda-lime glass are given in [3], where it was found that an empirical expression which adequately describes this slow crack growth behaviour is given by

$$\frac{dl}{dt} = V_0 \exp\left[(CK_I - E)/RT\right] \quad (13)$$

where l is the crack length, K_I the stress intensity factor, $E = 1.088 \times 10^5 \text{J mol}^{-1}$ (the activation energy), $R = 8.32 \text{J mol}^{-1}$ and $T = 298 \text{K}$. For soda-lime glass the crack growth data can be described by a bilinear curve fit between a fatigue limit $K_T = 2.49 \times 10^5 \text{N m}^{-3/2}$ and the critical stress intensity factor, $K_{IC} = 7.49 \times 10^5 \text{N m}^{-3/2}$. For the two regions, V_0 and C in Equation 13 are:

$$\ln V_0 = -1.08,\ C = 0.188,\ K_I < 3.62 \times 10^5 \text{N m}^{-3/2} \quad (14)$$

$$\ln V_0 = 10.3,\ C = 0.110,\ K_I > 3.62 \times \text{N m}^{-3/2} \quad (15)$$

(Note that in [8] there is a misprint concerning these constants.)

The results in this paper are reported in a manner similar to the flat plate solutions given in [8]. Fig. 5 shows results for stable crack growth where the initial crack length l_i is just sufficient to permit the crack to grow, i.e., Equation 8 is satisfied and thus $l_i = l_1$ (see inset in Fig. 5). The dashed line labelled l_1/h is a plot of this smallest initial crack length (ordinate on the right-hand side) as a function of the magnitude of the surface compressive stress σ_s (abscissa). For surface compression above a certain critical value σ_c the crack will grow in a stable manner to a length l_2 (see inset) upon which the critical stress intensity factor will be attained and sudden failure will occur. In Fig. 5 the time to failure T_f (in days) as well as the crack length l_2 is plotted.

For surface compression below σ_c, yet greater than the minimum threshold level σ_T which is necessary for crack growth, the crack will grow in a stable manner by first accelerating and then decelerating as the stress intensity factor decreases (see inset). The crack length l_a at which the crack arrests, i.e. $K_I = K_T$, as well as the time for this crack arrest to occur is shown in Fig. 5 as a function of the magnitude of the surface compression. It can be seen that the final arrested length of the crack will be greater than 75% of the cylinder wall thickness. As would be expected for these minimum size cracks, the time for crack arrest will increase asymptotically to infinity for surface compression magnitudes approaching σ_T.

The time to failure for crack lengths greater than the smallest value which will propagate, l_1, is plotted in Fig. 6. In this figure the time to failure in seconds is plotted as a function of the initial crack length l_i for different values of the surface compression stress σ_s. In comparison with the time to failure for the flat plate given in [8], it can be seen that for the particular $a:b$ ratio ($a:b = 0.9$) used in this numerical example, the time to failure for the hollow cylinder is very similar. Note that in [8] the time to failure is mislabelled.

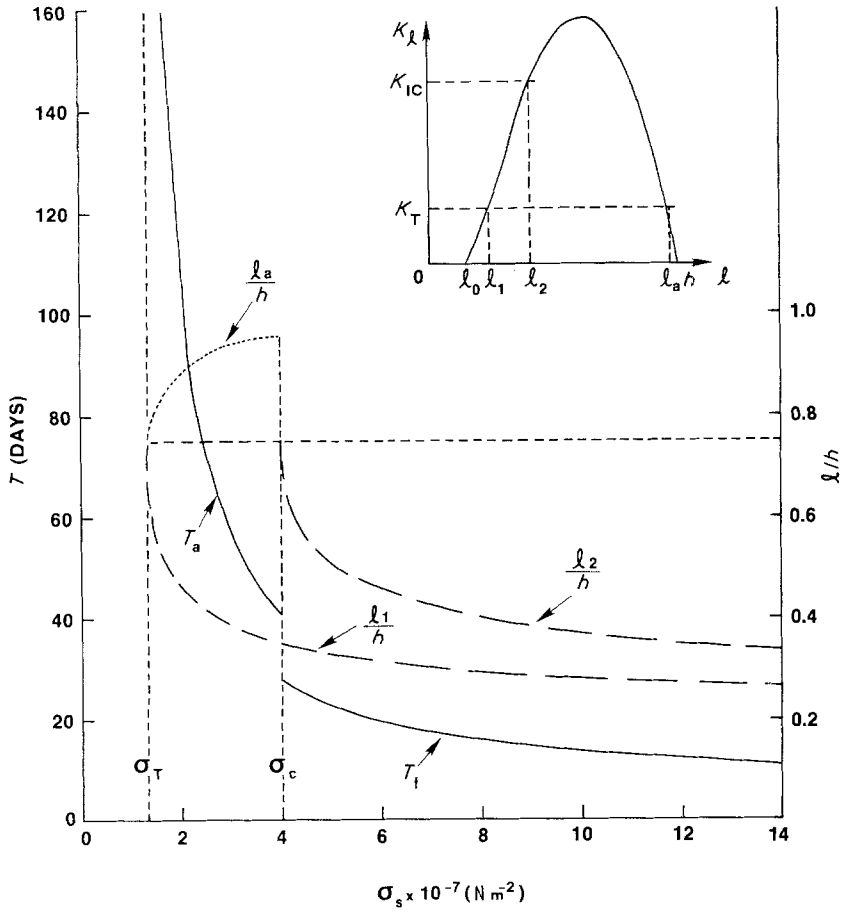

Figure 5 Time to failure T_f and time to arrest T_a for minimum size crack l_1 which exceeds K_T. Soda-lime glass 4 cm diameter cylinder exposed to water. $h = 2$ mm.

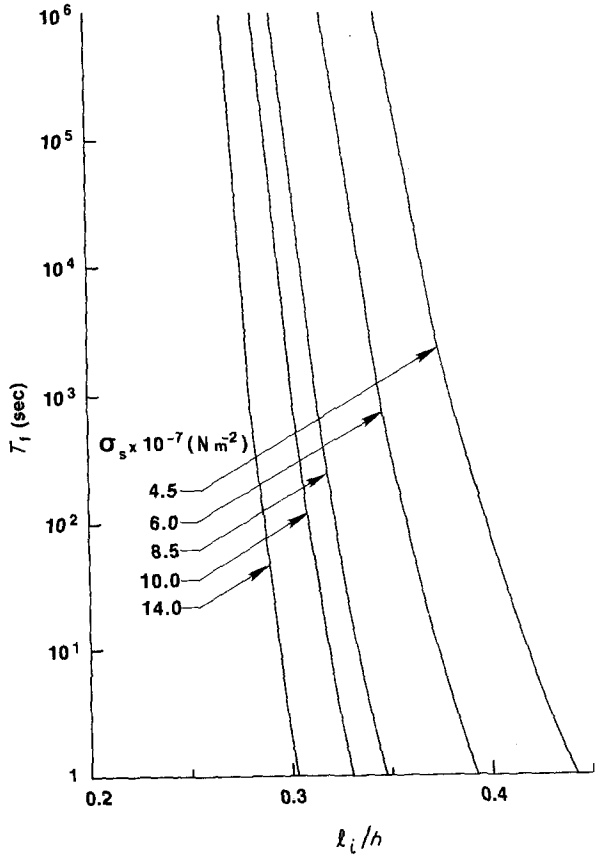

Figure 6 Time-to-failure in a 4 cm diameter, 2 mm thick soda-lime glass cylinder as a function of the initial crack length l_i for various values of surface compression σ_s.

5. Conclusion

The numerical results presented in this paper indicate that for a surface compression strengthened hollow cylinder, static fatigue leading to spontaneous failure in the absence of any external loading is indeed a plausible failure mechanism. This reinforces the conclusions drawn in [8] regarding static fatigue in a flat plate. As indicated in Fig. 6, this static fatigue behaviour for reasonable values of surface compression can result in failures due to fracture in a short period of time.

Even though it is often highly desirable to strengthen glasses by introducing compressive residual stresses at the structure surface, it should be recognized that this strengthening mechanism can lead to delayed failure if a surface crack is introduced that penetrates this protective zone. Cracks of this type can occur following foreign object impact and are generally very difficult to detect.

Since the crack growth velocities measured in glasses and ceramics are a sensitive function of the stress intensity factor, it is essential that this value be calculated accurately for the internal residual stress of interest. For structures that are in self-equilibrium this invariably means that a non-linear calculation must be performed to account for the crack surface contact which occurs for a portion of the crack surface in the compression strengthened zone. As demonstrated in [8] for a flat plate and in this paper for a hollow cylinder, calculations for the stress intensity factors and subsequently the stable crack growth behaviour can be developed from the solutions for embedded cracks.

References

1. R. J. CHARLES, *J. Appl. Phys.* **29** (1958) 1549.
2. *Idem, ibid.* **29** (1958) 1554.
3. S. M. WIEDERHORN and L. H. BOLZ, *J. Amer. Ceram. Soc.* **53** (1970) 543.
4. S. M. WIEDERHORN, H. JOHNSON, A. M. DINESS and A. H. HEUER, *ibid.* **57** (1974) 336.
5. A. G. EVANS, *J. Mater. Sci.* **7** (1972) 1137.
6. R. BADALIANCE, D. A. KROHN and D. P. H. HASSELMAN, *J. Amer. Ceram. Soc.* **57** (1974) 432.
7. D. P. H. HASSELMAN, R. BADALIANCE, K. R. KcKINNEY and C. H. KIM, *J. Mater. Sci.* **11** (1976) 458.
8. M. BAKIOGLU, F. ERDOGAN and D. P. H. HASSELMAN, *ibid.* **11** (1976) 1826.
9. R. ERDOL and F. ERDOGAN, *J. Appl. Mech.* **45** (1978) 281.
10. H. F. NIED and F. ERDOGAN, *Int. J. Fract.* **22** (1983) 277.

Received 26 November 1985
and accepted 17 January 1986